



Research Article

A comparative analysis of sequential and integrated optimization models for ship refueling operations

Tianfang Ma¹, Wei Wang^{2,*}, Xuecheng Tian¹ and Yan Liu¹

¹ Department of Logistics and Maritime Studies, The Hong Kong Polytechnic University, Hong Kong

² Business School, Sichuan University, Chengdu 610000, China

* **Correspondence:** wangwei_2025@scu.edu.cn.

Abstract: Maritime transportation underpins global trade and supply chains, with bunker fuel comprising a major share of voyage operating costs. Optimizing ship refueling is thus critical for improving energy efficiency and reducing expenses. A common sequential (two-stage) framework first derives a cost-minimal bunkering plan and then maximizes profit from cargo flows under that plan. Yet, this decoupled approach often yields suboptimal solutions, as refueling and container decisions are optimized separately. We develop an integrated one-stage model that simultaneously optimizes refueling and container flows on fixed liner services, comparing it to the two-stage model on stylized, industry-calibrated networks of 3, 8, and 15 ports. Results reveal consistent profit superiority for the integrated model, with gaps expanding alongside network scale and complexity (1.02% for 3 ports to 12.99% for 15 ports). Sensitivity tests on fuel-tank capacity, revenue levels, and local fuel price shocks affirm robustness, with gains amplifying under high demand or capacity constraints. Although the two-stage model provides modular transparency, the integrated formulation better balances fuel costs and cargo revenues, delivering substantial economic benefits in complex, constrained settings. Both models solve to optimality in seconds to minutes on standard hardware for tested instances, underscoring the integrated model's viability as a tactical decision tool. Overall, findings illuminate refueling optimization dynamics, quantify the inefficiency of bunker-first sequencing, and advise adopting integrated methods for larger networks.

Keywords: integrated model; two-stage model; ship refueling; liner shipping; bunker management; optimization

1. Introduction

Maritime transportation carries the majority of world trade and plays a central role in global supply chains. The sector is simultaneously under pressure to improve economic efficiency, reduce emissions, and enhance the resilience of logistics systems in the face of demand fluctuations and regulatory change. Li et al. propose an intelligent hyperheuristic for berth allocation and scheduling at marine container terminals, illustrating the role of optimization in improving port-side operational efficiency [1], while Mollaoglu et al. review maritime transportation research through the lens of the sustainable development goals, emphasizing sustainability and decarbonization-related research directions [2]. Within this broader context, bunker fuel management remains one of the key levers for liner operators to influence both cost and emissions footprints.

Given that bunker costs constitute a substantial proportion of voyage operating expenditures, their optimization directly influences liner shipping profitability and compliance with increasingly stringent emissions regulations. A central modeling question is how to represent the interaction between refueling and revenue-generating activities. One widely used approach is a sequential (i.e., two-stage) decision framework, which prioritizes fuel cost minimization before revenue planning. An alternative is an integrated (i.e., one-stage) formulation that simultaneously optimizes bunkering and container routing at the network level. This paper focuses on a systematic comparative analysis of these two paradigms, evaluating their efficacy in profit maximization across varying network scales and operational conditions, and deriving prescriptive insights for model selection based on problem structure and strategic priorities.

Relative to integrated approaches discussed in the broader literature, our integrated formulation is deliberately parsimonious and tailored to the bunker–cargo setting studied here. It embeds refueling decisions and origin–destination flows for a fixed liner service network into a single profit-maximizing linear program, with explicit coupling between fuel inventories, tank capacity, and slot/weight constraints on each leg. The main methodological focus of the paper is therefore not on introducing an entirely new modeling primitive, but on positioning this profit-based integrated formulation side by side with the widely used two-stage benchmark and quantifying the economic consequences of choosing one structure over the other.

This paper makes three contributions. First, we formalize and contrast the two modeling paradigms within a consistent mathematical and experimental framework, highlighting their structural differences and implications. In particular, the integrated model is constructed as the profit-maximizing, network-level counterpart of the classical two-stage refueling–then–stowage logic, rather than a reimplementing of integrated designs that target other planning layers. Second, we provide a rigorous empirical evaluation across a spectrum of network complexities (3, 8, and 15 ports), assessing performance not only on optimality gaps but also on scalability, robustness and solution times. Third, through extensive sensitivity analyses, we quantify how the value of integration is modulated by key operational parameters, including fuel tank capacity, cargo revenue structures, and port-specific price shocks, thereby offering actionable guidance for implementation and clarifying the conditions under which sequential planning is acceptable from an economic perspective.

The rest of the paper is organized as follows. Section 2 reviews related work on ship refueling, liner network planning and integrated bunker–cargo optimization. Section 3 presents the problem statement and model formulations. Section 4 describes the experimental design and reports numerical results. Section 5 concludes and outlines directions for future research.

2. Literature review

Research on ship refueling and bunker management has evolved along two primary dimensions: modeling scope and treatment of uncertainty. Related optimization work in other application domains has similarly emphasized the trade-off between model fidelity and tractability: Ala and Goli integrate machine learning with optimization for fair operating-room assignment [3], while Attari et al. develop a gravitational meta-heuristic for resource-constrained project scheduling [4], both illustrating how computational approaches balance solution quality and efficiency. A substantial stream of work focuses on deterministic, cost-centric approaches. Besbes and Savin study joint route selection and refueling under a cost-driven objective [5], and Fagerholt et al. optimize operational decisions (e.g., speed) to reduce fuel use and emissions [6]. While providing essential methodological foundations and practical heuristics, these approaches often segregate refueling decisions from the revenue-generation process: container flows and commercial priorities are either predetermined or represented through simple exogenous constraints.

A second, more advanced stream introduces stochastic elements, principally addressing fuel price volatility through stochastic programming or robust optimization frameworks. Wang and Meng formulate robust bunker management for liner shipping networks under fuel-price uncertainty [7], while Wang et al. provide an overview of green development in the maritime industry and summarize research perspectives that motivate uncertainty-aware planning [8]. This line of inquiry enhances decision robustness by hedging against uncertain bunker prices and, in some cases, demand, but frequently retains a cost-minimization objective and continues to treat container flows as exogenously determined or only loosely coupled to bunkering choices. In parallel, the literature on liner shipping network design and schedule robustness has developed models that incorporate frequency, transshipment, and schedule-reliability considerations: Meng and Wang address service network design with empty-container repositioning [9], Wang et al. incorporate delivery deadlines in network design [10], and Wang and Meng propose robust schedule design for liner services [11]; however, bunker procurement is often handled through simplified cost parameters.

Acknowledging the interplay between speed, consumption and schedule, a third category of partially integrated approaches has emerged. Ronen analyzes how oil price affects optimal ship speed [12], Halvorsen-Weare et al. study fleet composition and periodic routing decisions [13], Du et al. develop two-phase solutions for ship speed and trim optimization [14], and Psaraftis and Kontovas provide a taxonomy and survey of speed models for energy-efficient maritime transportation [15]. Empirical results from these studies demonstrate tangible benefits. For example, Meng and Wang show how network-level operational decisions can drive cost outcomes in liner systems [9], and Korsvik et al. develop a tabu search heuristic for ship routing and scheduling that improves operational feasibility under complex constraints [16]. However, a common limitation persists: container transport demand and associated revenues are largely treated as predetermined inputs. Consequently, the fundamental economic trade-off between strategic fuel inventory management and tactical revenue maximization via cargo allocation remains inadequately captured.

Within this landscape, sequential two-stage structures remain common in practice and in the academic literature. Zhen et al. develop a dynamic-programming approach for optimal ship refueling decisions [17], and Wang et al. provide a critical review of bunker consumption optimization methods [18], both reflecting the prevalence of bunker-first or cost-centric planning logic. In such

models, a cost-optimal bunkering plan is determined first; subsequently, with fuel variables fixed, a second model allocates containers and computes revenue. This decomposition offers computational and organizational modularity, such as separating bunker procurement from commercial planning. In related applied optimization settings, Xie et al. use a scenario-based planning structure to decouple decision layers in a coupled infrastructure system [19], and Gerres et al. review cross-sector decarbonisation potentials that similarly motivate modular planning across interacting operational subsystems [20]. However, such modularity intrinsically risks suboptimality by neglecting the bidirectional feedback between bunkering choices and profitable cargo routing opportunities. Zhen et al. emphasize that refueling decisions depend on route-level dynamics and constraints [17], while Fan et al. analyze how congestion and port expansion shape competitive outcomes in container imports [21], underscoring that operational conditions and capacity frictions can materially affect revenue opportunities that a sequential approach may not capture well.

Integrated formulations that couple bunker, speed, and network decisions in a single model have also been discussed in broader contexts. Plum et al. study bunker purchasing under contracts, capturing procurement structure within a unified decision framework [22], and Wang et al. integrate network design decisions with service deadlines [10], illustrating how joint formulations can internalize cross-component trade-offs. These formulations conceptually capture the opportunity cost of using ship weight and capacity for fuel versus revenue-generating cargo, a trade-off particularly salient in complex networks with multifaceted routing and refueling options. However, most existing integrated models either target different planning problems (e.g., integrated network design and service reliability) or embed bunkering within higher-level design decisions, making it difficult to isolate the economic value of integration in the bunker–cargo space itself.

Against this background, the present paper fills a specific gap. Devarapali et al. provide a detailed analysis of electric tugboat deployment in maritime transportation [23], reflecting the broader move toward integrated operational assessment in maritime systems; however, systematic and controlled comparisons that isolate the economic value of integrating bunkering with cargo-flow decisions on a fixed liner network remain limited. We develop a linear profit-maximizing integrated model that explicitly couples bunker decisions with origin–destination flows on a fixed network, and we compare it systematically with a two-stage benchmark that mirrors common practice in liner operations. By holding many modeling features constant (deterministic demands and prices, fixed port rotations, and vessel capacities), we isolate the effect of the modeling structure on economic performance. The contribution is therefore twofold: we provide a transparent, network-level integrated bunker–cargo formulation and, more importantly, quantify the profit lost when bunker-first, cost-minimizing policies are used in settings where weight and capacity constraints bind.

3. Problem statement and mathematical model

This section describes the studied problem. We list needed notations in Table 1.

Table 1. Notations.

Notation	Description
Sets and indices	
$\mathbf{P} = \{1, \dots, P\}$	Set of physical ports, indexed by o, d .
$\mathbf{R} = \{1, \dots, R\}$	Set of shipping routes, indexed by r .
$\mathbf{I}_r = \{1, \dots, I_r\}$	Set of ports of call on route r ($r \in \mathbf{R}$), indexed by i, j, k .
Parameters	
p_{ri}	Physical port corresponding to the i -th port of call on route r ($r \in \mathbf{R}$).
u_{ri}	Fuel consumption (ton) of the sailing from the i -th port of call to the $(i + 1)$ -st on route r .
$c_{p_{ri}}$	Fuel price at the i -th port of call on route r .
e_{od}	Revenue of shipping a container from port o to port d .
q_{od}	Container demand from port o to port d .
V_r	Total deadweight capacity (tons) of the ship deployed on route r .
V_r^T	Fuel tank capacity (tons) of the ship deployed on route r .
V_r^C	Maximum number of containers onboard the ship deployed on route r .
δ_{rijk}	Binary parameter indicating whether a container transported from the i -th port of call to the j -th port of call on route r is onboard ($\delta_{rijk} = 1$) during the voyage from the k -th port of call to the next, and $\delta_{rijk} = 0$ otherwise.
ζ_r	Initial amount of fuel of the container ship on route r ($r \in \mathbf{R}$).
W	Weight of each container.
Decision variables	
y_{ri}	Amount of fuel bunkered at the i -th port of call on route r .
z_{ri}	Amount of fuel in the bunker tank upon arrival at the i -th port of call on route r before refueling.
x_{od}	Number of containers transported from port o to port d .
x_{rij}	Number of containers transported from the i -th to the j -th port of call on route r .

We consider a container ship that earns profit by transporting containers between ports. There are P ports in total, and the fuel price (US dollars per ton) at port p is denoted by c_p ($p \in \mathbf{P}$). There are R weekly service routes, each forming a loop. For each route $r \in \mathbf{R}$, there are I_r ports of call, which correspond to physical ports denoted by p_{r1}, \dots, p_{rI_r} in the network. The fuel consumption (tons) of the sailing from the i -th port of call to the $(i + 1)$ -st on route r is u_{ri} ($r \in \mathbf{R}, i \in \mathbf{I}_r$); in particular, u_{rI_r} is the fuel consumption from the I_r -th port of call back to the first. The total deadweight capacity (tons) of the container ship deployed on route r is V_r , and the fuel tank capacity (tons) is V_r^T . Each container weighs W tons, and the maximum number of containers onboard is V_r^C ($r \in \mathbf{R}$).

We consider the shipping process for the container ship. The container demand from port o ($o \in \mathbf{P}$) to port d ($d \in \mathbf{P}, d \neq o$) is q_{od} (container/week) and the revenue of shipping a container from o to d is e_{od} (US dollars/container). The parameter δ_{rijk} ($r \in \mathbf{R}, i, j, k \in \mathbf{I}_r, i \neq j$) indicates whether a container transported from the i -th port of call to the j -th port of call on route r is onboard on the voyage from the k -th port of call to the next. Specifically, $\delta_{rijk} = 1$ if the container mentioned above is onboard from the k -th port of call to the $(k + 1)$ -st port of call and $\delta_{rijk} = 0$ otherwise. The decision variable x_{rij}

($r \in \mathbf{R}, i, j \in \mathbf{I}_r, i \neq j$) represents how many containers to transport from the i -th port of call to the j -th port of call on route r , and x_{od} ($o, d \in \mathbf{P}, d \neq o$) denotes how many containers to transport from port o to port d . The variable y_{ri} ($r \in \mathbf{R}, i \in \mathbf{I}_r$) represents the amount of fuel bunkered at the i -th port of call on route r , and z_{ri} ($r \in \mathbf{R}, i \in \mathbf{I}_r$) denotes the amount of fuel in the bunker tank when a ship arrives at the i -th port of call on route r before refueling.

By construction, x_{rij} indexes the flow of containers between ports of call i and j along route r (with $i \neq j$); it does not correspond to a single sailing leg. Leg-specific onboard volumes are obtained by combining these flows with the incidence parameters δ_{rijk} in the capacity constraints below: for each leg between the k -th and $(k + 1)$ -st ports of call, δ_{rijk} identifies whether a container travelling from i to j is on board that leg.

The objective of this study is to maximize the profit of the container ship, calculated as transport revenue minus the cost of fuel consumption.

In practice, many liner operators treat fuel cost and revenue decisions sequentially. A two-stage framework first computes a cost-minimizing refueling plan and then treats this plan as fixed when determining container flows. The following mathematical models [M0] and [M1] formalize this two-stage logic in our setting.

[M0]

$$\min \sum_{r=1}^R \sum_{i=1}^{I_r} c_{pri} y_{ri}, \quad (3.1)$$

$$\text{s.t. } z_{ri} + y_{ri} \leq V_r^T \quad r \in \mathbf{R}, i \in \mathbf{I}_r, \quad (3.2)$$

$$z_{r,i+1} = z_{ri} + y_{ri} - u_{ri} \quad r \in \mathbf{R}, i = 1, \dots, I_r - 1, \quad (3.3)$$

$$z_{r1} = \zeta_r \quad r \in \mathbf{R}, \quad (3.4)$$

$$z_{r,I_r+1} = z_{rI_r} + y_{rI_r} - u_{rI_r} \quad r \in \mathbf{R}, \quad (3.5)$$

$$y_{ri} \geq 0 \quad r \in \mathbf{R}, i \in \mathbf{I}_r, \quad (3.6)$$

$$z_{ri} \geq 0 \quad r \in \mathbf{R}, i \in \mathbf{I}_r. \quad (3.7)$$

Objective function (3.1) minimizes the total cost that the container ship spends on fuel consumption. Constraints (3.2) enforce that the sum of the amount of fuel bunkered at the i -th port of call on route r and the amount of fuel in the bunker tank upon arrival at that port before refueling cannot exceed the fuel-tank capacity V_r^T . Constraints (3.3) describe the fuel-balance evolution between successive ports of call. Constraint (3.4) specifies the initial amount of fuel. Constraint (3.5) determines the fuel level when the ship returns to the first port of call. Constraints (3.6) and (3.8) enforce nonnegativity of bunkering and inventory variables.

For the two-stage model, [M0] constitutes the first stage, which determines the optimal refueling plan by minimizing fuel cost. Let \hat{c} denote the minimum fuel cost obtained from [M0]. In addition, let \hat{z}_{rk} and \hat{y}_{rk} be the optimal fuel-on-arrival and bunkering quantities at the k -th port of call on route r obtained from [M0]. These values are then treated as fixed input in the second stage, which is defined as follows.

[M1]

$$\max \sum_{o \in \mathbf{P}} \sum_{d \in \mathbf{P}} e_{od} x_{od} - \hat{c} \quad (3.8)$$

$$\text{s.t. } x_{od} = \sum_{r=1}^R \sum_{i=1, p_{ri}=o}^{I_r} \sum_{j=1, p_{rj}=d}^{I_r} x_{rij}, \quad o, d \in \mathbf{P}, \quad (3.9)$$

$$x_{od} \leq q_{od}, \quad o, d \in \mathbf{P}, \quad (3.10)$$

$$\sum_{i=1}^{I_r} \sum_{j=1}^{I_r} \delta_{rijk} x_{rij} \leq V_r^C, \quad r \in \mathbf{R}, k \in \mathbf{I}_r, \quad (3.11)$$

$$W \cdot \left(\sum_{i=1}^{I_r} \sum_{j=1}^{I_r} \delta_{rijk} x_{rij} \right) + \hat{z}_{rk} + \hat{y}_{rk} \leq V_r, \quad r \in \mathbf{R}, k \in \mathbf{I}_r, \quad (3.12)$$

$$x_{rij} \geq 0, \quad r \in \mathbf{R}, i, j \in \mathbf{I}_r, \quad (3.13)$$

$$x_{od} \geq 0, \quad o, d \in \mathbf{P}. \quad (3.14)$$

$$(3.15)$$

The objective function (3.8) maximizes container ship profit, calculated as transport revenue minus fixed fuel costs predetermined by model [M0]. Constraint (3.9) ensures that, for each origin–destination pair, the transported container volume equals the sum of containers moved between corresponding port-of-call pairs across all routes. Constraint (3.10) enforces that the number of containers transported from port o to port d does not exceed demand for any origin–destination pair. Constraint (3.11) limits the number of containers on board during any leg of a route so that the ship’s container-slot capacity is not exceeded. Constraint (3.12) enforces the deadweight constraint by requiring that the combined weight of containers and fuel never surpasses V_r on any leg. Finally, Constraints (3.13) and (3.14) enforce nonnegativity for all decision variables x_{rij} and x_{od} , respectively.

Although the two-stage model has been widely used in practice, its solutions may be economically suboptimal because only one part of the decision space is optimized at a time. Treating fuel cost minimization and revenue maximization in isolation can reduce the value of the resulting plans in real operations. To address this issue, we introduce an integrated model that uses a single formulation to consider both fuel-consumption costs and shipping revenues, as presented below.

[M2]

$$\max \sum_{o \in \mathbf{P}} \sum_{d \in \mathbf{P}} e_{od} x_{od} - \sum_{r=1}^R \sum_{i=1}^{I_r} c_{p_{ri}} y_{ri} \quad (3.16)$$

$$\text{s.t. } x_{od} = \sum_{r=1}^R \sum_{i=1, p_{ri}=o}^{I_r} \sum_{j=1, p_{rj}=d}^{I_r} x_{rij} \quad o, d \in \mathbf{P}, \quad (3.17)$$

$$x_{od} \leq q_{od} \quad o, d \in \mathbf{P}, \quad (3.18)$$

$$z_{ri} + y_{ri} \leq V_r^T \quad r \in \mathbf{R}, i \in \mathbf{I}_r, \quad (3.19)$$

$$z_{r,i+1} = z_{ri} + y_{ri} - u_{ri} \quad r \in \mathbf{R}, i = 1, \dots, I_r - 1, \quad (3.20)$$

$$z_{r1} = \zeta_r \quad r \in \mathbf{R}, \quad (3.21)$$

$$z_{r,I_r+1} = z_{rI_r} + y_{rI_r} - u_{rI_r} \quad r \in \mathbf{R}, \quad (3.22)$$

$$\sum_{i=1}^{I_r} \sum_{j=1}^{I_r} \delta_{rijk} x_{rij} \leq V_r^C \quad r \in \mathbf{R}, k \in \mathbf{I}_r, \quad (3.23)$$

$$W \cdot \left(\sum_{i=1}^{I_r} \sum_{j=1}^{I_r} \delta_{rijk} x_{rij} \right) + z_{rk} + y_{rk} \leq V_r \quad r \in \mathbf{R}, k \in \mathbf{I}_r, \quad (3.24)$$

$$x_{rij} \geq 0 \quad r \in \mathbf{R}, i, j \in \mathbf{I}_r, \quad (3.25)$$

$$y_{ri} \geq 0 \quad r \in \mathbf{R}, i \in \mathbf{I}_r, \quad (3.26)$$

$$z_{ri} \geq 0 \quad r \in \mathbf{R}, i \in \mathbf{I}_r, \quad (3.27)$$

$$x_{od} \geq 0 \quad o, d \in \mathbf{P}. \quad (3.28)$$

The objective function (3.16) maximizes container ship profit, calculated as transport revenue minus refueling costs at ports of call. The interpretations of Constraints (3.17)–(3.28) parallel those of models [M0] and [M1], with the key difference that refueling and cargo flows are now optimized jointly rather than sequentially. Compared with the two-stage model, the integrated model increases internal consistency between refueling and stowage decisions and explicitly captures the opportunity cost of using weight and slots for fuel rather than for containers.

4. Experiments

4.1. Experiment descriptions

We evaluate the two-stage model and the integrated model across three instances with 3, 8, and 15 ports to assess scalability and performance in optimizing fuel procurement and container transport. Each instance includes two routes with different port sequences, reflecting realistic shipping operations.

The experimental setup comprises three distinct instances with progressively increasing complexity. The 3-port instance features ports A, B, and C with two distinct routing patterns. Route 1 follows the sequence $A \rightarrow B \rightarrow C$, while Route 2 employs another routing pattern $A \rightarrow C \rightarrow B$, creating complementary coverage of the three ports. Fuel prices are set at \$500 per ton for port A, \$750 per ton for port B, and \$750 per ton for port C. All other parameters include container weight of 12 tons per TEU, ship capacity of 7000 tons per leg, fuel-tank capacity of 2000 tons, container-slot capacity of 500 TEU, and fuel consumption ranging 400–450 tons per leg.

The 8-port instance expands the network to include ports A through H with distinct route configurations: Route 1 sequentially visits all eight ports ($A \rightarrow B \rightarrow C \rightarrow D \rightarrow E \rightarrow F \rightarrow G \rightarrow H$), while Route 2 adopts an alternating pattern ($A \rightarrow C \rightarrow E \rightarrow G \rightarrow B \rightarrow D \rightarrow F \rightarrow H$). Capacity parameters remain consistent with the 3-port instance, featuring 12-ton TEUs, 7000-ton ship capacity per leg, 2000-ton fuel-tank capacity, and 500-TEU container-slot limits. Fuel consumption per leg follows a cyclical pattern based on the leg's sequence position in each route: for a leg at position i (where i starts from 1), consumption is calculated as $360 + 20 \cdot ((i - 1)/5)$ tons, resulting in a repeating sequence of 360, 380, 400, 420, and 440 tons every five legs. For the eight-leg routes, this yields a consumption sequence of 360, 380, 400, 420, 440, 360, 380, and 400 tons per route. Meanwhile, fuel prices are set to increase progressively from \$500 to \$745 per ton in 35-dollar increments across the eight ports, creating a structured testing environment for evaluating bunkering optimization strategies in moderately complex networks.

The 15-port instance expands the network to include ports A through O with distinct route configurations: Route 1 sequentially visits all fifteen ports ($A \rightarrow B \rightarrow C \rightarrow D \rightarrow E \rightarrow F \rightarrow G \rightarrow H \rightarrow I \rightarrow J \rightarrow K \rightarrow L \rightarrow M \rightarrow N \rightarrow O$), while Route 2 adopts an alternating pattern covering odd-indexed ports first followed by even-indexed ports ($A \rightarrow C \rightarrow E \rightarrow G \rightarrow I \rightarrow K \rightarrow M \rightarrow O \rightarrow B \rightarrow D \rightarrow F \rightarrow H \rightarrow$

$J \rightarrow L \rightarrow N$). Capacity parameters remain consistent with the 3-port instance, featuring 12-ton TEUs, 7000-ton ship capacity per leg, 2000-ton fuel-tank capacity, and 500-TEU container-slot limits. Fuel consumption follows a cyclical pattern of 360–440 tons per leg, while fuel prices increase progressively from \$500 to \$990 per ton in 35-dollar increments across the fifteen ports.

All instances feature origin–destination-specific demands ranging from 450–600 TEU, with revenues calculated based on distance between ports plus premiums for long-haul transport. These input ranges are stylized but chosen to be consistent with typical bunker prices, vessel capacities, and utilization levels reported in the liner shipping literature, so that the instances serve as industry-relevant proof-of-concept test beds rather than purely abstract toy examples. Figure 1 provides a visual overview of the stylized networks and route patterns used in the experiments.

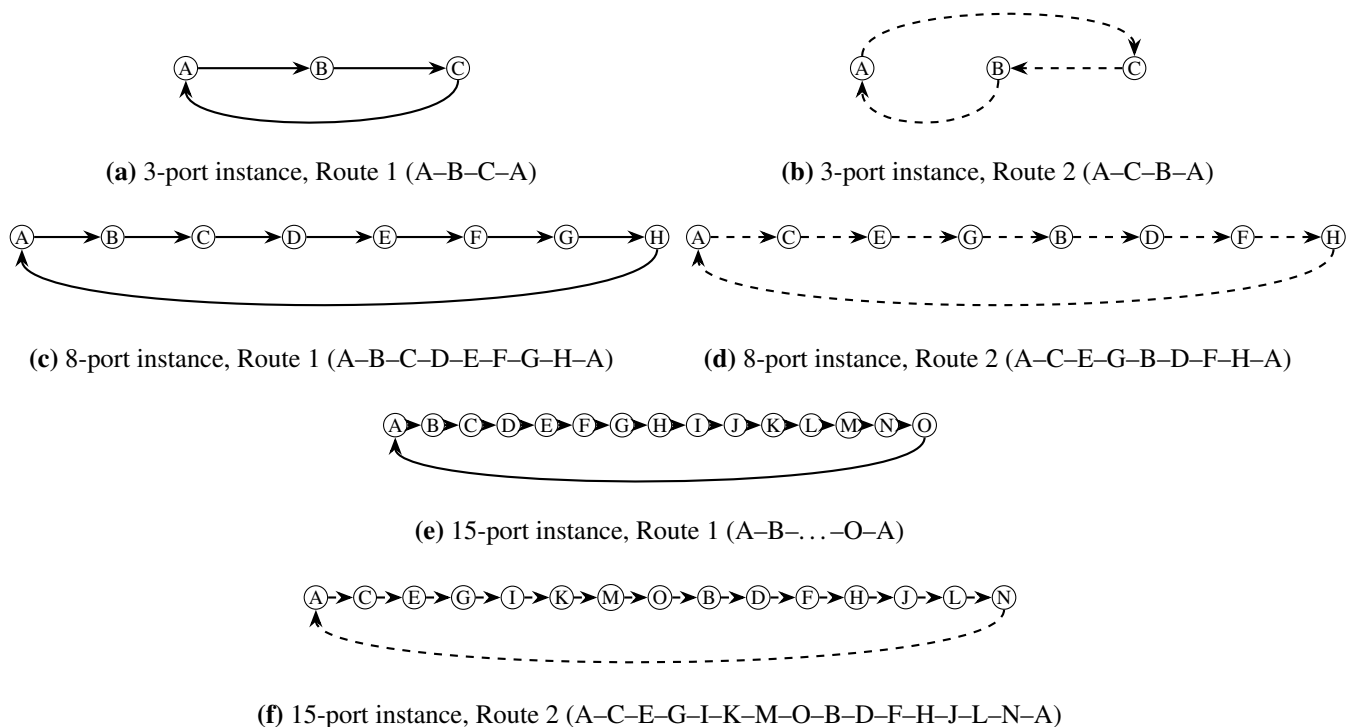


Figure 1. Stylized route structures for the three benchmark instances. Each subfigure shows a single service route with ports represented as circular nodes and arrows indicating the visiting sequence. Solid lines correspond to Route 1 and dashed lines to Route 2, with layouts chosen to avoid overlaps between nodes, links, and labels.

4.2. Experimental results

4.2.1. Performance comparison across instances

Table 2 summarizes the key performance metrics for both models across the three instances. The integrated model demonstrates consistent profit advantages over the two-stage approach, with the improvement magnitude increasing substantially with instance size. This scalability advantage arises because larger networks provide more opportunities for the integrated model to optimize the trade-off between fuel costs and container revenues simultaneously. The performance gap exhibits a clear scaling pattern: from a modest 1.02% improvement in the 3-port instance to significant advantages of 9.17%

and 12.99% in the 8-port and 15-port instances, respectively.

In the 3-port instance, the relatively constrained decision space limits the integrated model's opportunity for substantial improvements. However, as the network expands to 8 and 15 ports, the combinatorial possibilities for coordinating bunkering and container operations grow rapidly. The integrated model leverages this expanded decision space to make strategic trade-offs that are invisible to the sequential two-stage approach.

The underlying mechanism driving this performance divergence lies in the integrated model's ability to make strategic bunkering decisions that support optimal container routing. While the two-stage model commits to a fuel procurement plan before considering container assignments, the integrated model dynamically adjusts bunkering to accommodate high-value container flows, even if this requires purchasing more expensive fuel at intermediate ports. This flexibility proves increasingly valuable as network complexity grows, explaining the observed scalability advantage.

From a financial perspective, the observed profit improvements are not marginal. In liner shipping, bunker costs typically account for a large share of voyage operating expenditures, and reported EBIT margins often fall in the single-digit percentage range of revenue. Against this backdrop, profit uplifts of 5–13% in the larger test instances correspond to a material enhancement of voyage profitability rather than a negligible rounding error, especially when aggregated over multiple sailings and services. Figure 2 graphically compares the profit levels of the two formulations across the three instances, highlighting both the absolute and relative gaps.

Table 2. Overall performance comparison across instances (USD).

Instance	Model	Revenue	Fuel cost	Profit	Profit advantage	Improvement (%)
3-port	Two-stage	11,715,400	950,000	10,765,400	—	—
	integrated	11,900,000	1,025,000	10,875,000	109,600	1.02
8-port	Two-stage	33,614,100	3,061,100	30,553,000	—	—
	integrated	36,700,000	3,345,300	33,354,700	2,801,700	9.17
15-port	Two-stage	63,530,000	6,937,500	56,592,500	—	—
	integrated	71,900,000	7,957,400	63,942,600	7,350,100	12.99

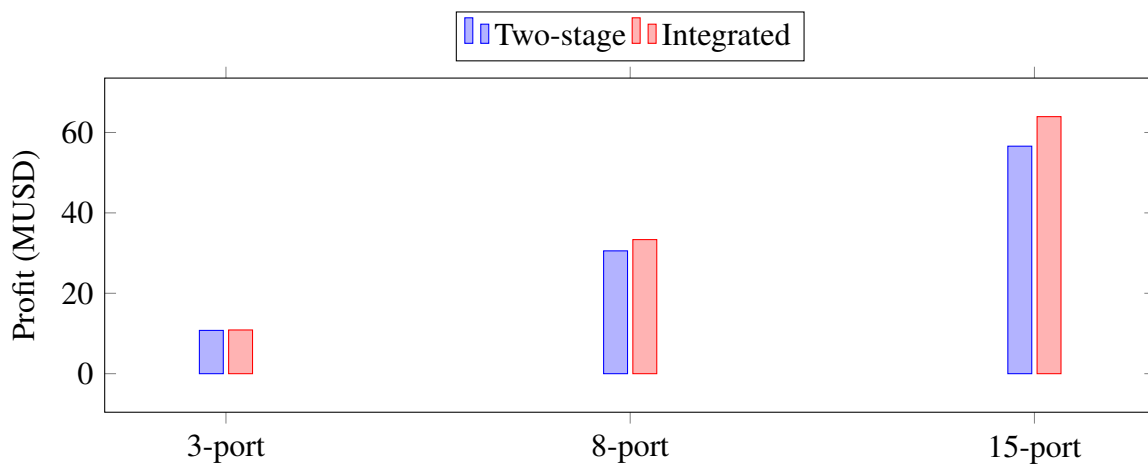


Figure 2. Profit comparison between the two-stage and integrated models for the three instances (values in millions of USD).

4.2.2. Managerial interpretation of refueling and routing patterns

While Table 2 and Figure 2 focus on aggregated revenue, fuel cost and profit, the two formulations differ markedly in the underlying refueling and routing patterns that generate these numbers. This subsection summarizes the main qualitative differences observed in the optimal solutions and highlights their managerial implications.

In the 3-port instance, both models adopt similar qualitative strategies: they bunker primarily at the cheapest port A and limit purchases at the more expensive ports B and C. The integrated model, however, slightly reduces the amount of fuel carried across the heaviest legs and uses the freed weight to transport additional containers on the most profitable origin–destination pairs. The resulting profit gain is modest but illustrates the basic mechanism: refueling decisions are adjusted just enough to avoid unnecessary fuel inventory on high-value legs.

In the 8-port instance, the patterns become more distinct. The two-stage model, which minimizes fuel cost in the first stage, tends to concentrate purchases at the cheapest ports early in each loop and then carry this fuel through multiple subsequent legs. This approach keeps fuel expenditure low but increases the ship's displacement on mid-route segments where several high-yield OD flows overlap. By contrast, the integrated model spreads bunkering more evenly across ports: it accepts slightly higher unit prices at some intermediate ports in order to reduce the amount of fuel that must be carried on the most capacity-critical legs. Operationally, this translates into higher slot utilization for long-haul OD pairs and a de-prioritization of lower-yield, shorter-haul flows that would otherwise occupy weight on those legs.

The 15-port instance amplifies these effects. With more ports and longer routes, the two-stage model's early, cost-driven bunkering decisions lock in substantial fuel inventories that are then transported across long stretches of the network. The integrated model instead times refueling to keep total load (containers plus fuel) closer to the deadweight limit on revenue-critical arcs while allowing more slack on less profitable segments. From a management standpoint, this behavior is consistent with a policy that coordinates bunker procurement with commercial priorities: rather than minimizing bunker cost in isolation, the liner operator accepts localized increases in fuel expenditure at specific ports in order to unlock additional revenue on key corridors.

These patterns suggest that the integrated model can be interpreted as an analytical support tool for joint bunker procurement and cargo allocation decisions. It indicates when a strict “bunker-at-the-cheapest-port” rule is suboptimal and when it is worthwhile to diversify purchases across ports to preserve capacity on important trade lanes.

4.2.3. Sensitivity analysis: 8-port instance

We assess robustness relative to the following baseline configuration: TEU weight = 12 t; ship weight capacity per leg = 7000 t; fuel-tank capacity = 2000 t; slot capacity = 500 TEU; port fuel prices (USD/t) at A–H equal to (500, 535, 570, 605, 640, 675, 710, 745); and per-cycle leg consumptions (t) equal to (360, 380, 400, 420, 440, 360, 380, 400). All inputs not explicitly varied are fixed at these baseline values. Three one-factor sensitivity experiments are conducted on the 8-port network and solved under the same modeling and computational settings as the baseline. For each experiment, we report network-level profits (aggregated over the two routes) for the *two-stage* and *integrated* models and show the outcomes in Table 3.

S1: Fuel-tank capacity V^T . We vary $V^T \in \{1200, 1600, 2000, 2400, 2800\}$ t to study how bunkering flexibility interacts with weight constraints. Both models benefit from larger tanks, yet the *integrated* model captures a wider margin as V^T grows: by coordinating fuel timing/quantity with cargo loading, it reduces weight interference on the heaviest legs and preserves capacity for high-yield OD flows. The advantage over *two-stage* expands from roughly 2.3 MUSD to 3.1 MUSD across the tested range.

S2: Global revenue scale α . We multiply all OD revenues by $\alpha \in \{0.8, 0.9, 1.0, 1.1, 1.2\}$. Profits scale nearly linearly for both models. However, *integrated* exhibits a consistently larger incremental gain between adjacent α levels because it reallocates slots toward the most profitable OD pairs and adjusts bunkering to free weight where those flows traverse multiple legs. At $\alpha = 1.0$, the gap remains sizeable and widens further as α increases.

S3: Localized price shock at port A only. We scale the fuel price at port A by a multiplier $\gamma \in \{0.8, 0.9, 1.0, 1.1, 1.2\}$ while keeping all other port prices at their baseline values. As γ increases, both models' profits decline. The *integrated* model mitigates this impact by shifting bunkering away from A when beneficial and rebalancing cargo to preserve high-margin OD flows. Across the tested range, the *integrated* model maintains a stable profit premium of roughly 2.6–3.0 MUSD.

Table 3. Sensitivity results on the 8-port network: network-level profit (MUSD).

S1: Tank capacity V_r^T (t)					
Model	1200	1600	2000	2400	2800
Two-stage	28.90	29.85	30.55	30.90	31.10
Integrated	31.20	32.40	33.35	33.90	34.20
S2: Revenue scale α					
Model	0.8	0.9	1.0	1.1	1.2
Two-stage	24.60	27.65	30.55	33.60	36.50
Integrated	26.90	30.15	33.35	36.70	39.90
S3: Price multiplier γ at A only					
Model	0.8	0.9	1.0	1.1	1.2
Two-stage	31.30	30.95	30.55	30.10	29.60
Integrated	34.20	33.80	33.35	32.95	32.60

S1 (Tank capacity). Increasing the per-leg tank capacity directly alleviates two operational frictions that mattered in the baseline: the risk of running into a tight tank limit on heavy-consumption legs and the loss of payload weight caused by carrying fuel across those same legs. When the tank is small (for example, 1200 t), the refueling plan is forced to “carry ahead” fuel into segments that already require 400–440 t of burn, which leaves less effective room for containers exactly where long multi-leg flows pass through. As the tank grows to 1600, 2000, 2400, and 2800 t, the model can postpone purchases to legs with more headroom and reduce the amount of fuel that must be transported over the heaviest arcs. The result is a monotone and concave increase in network profit for both optimization approaches in

Table 3: the two-stage model rises from 28.90 to 31.10 M USD and the integrated model rises from 31.20 to 34.20 M USD. By synchronizing the timing and size of fuel purchases with the pattern of container flows, the integrated formulation deliberately keeps the combined fuel load smaller on the legs that are both heavy and valuable for revenue. This coordination turns extra tank capacity into extra effective payload exactly where it is worth the most. Once the tank becomes large enough, both approaches exhibit diminishing returns because the remaining bottlenecks are the ship's weight limit and the container-slot limit; even then, the integrated model continues to realize a larger share of the remaining gains because its refueling plan adapts to the revenue map of the route.

S2 (Revenue scale). Scaling all origin–destination revenues by a common factor changes the value of every container but does not alter the pattern of fuel prices or leg consumptions. Under such an experiment, the most profitable corridors are the long-haul pairs that traverse many legs; these corridors put sustained pressure on both container slots and weight along their path. The two-stage model cannot respond on the fuel side because its refueling plan is fixed before cargo is assigned, so a portion of the additional revenue remains unrealized whenever the precommitted fuel load occupies weight on the critical legs. The integrated model adjusts both sides at once: it routes more containers through the high-yield corridors and, at the same time, re-times purchases so that less fuel needs to be carried across the legs that those flows traverse. This joint adjustment produces a steeper and nearly linear profit slope in Table 3. Around the baseline scale, each 10% increase in revenue adds roughly 2.95 M USD of profit for the two-stage model but about 3.25 M USD for the integrated model. The absolute premium therefore widens as the market improves, growing from approximately 2.30 M USD at a scale of 0.8 to approximately 3.40 M USD at a scale of 1.2. From a managerial point of view, this means that in stronger demand regimes the simultaneous approach captures more upside because it not only sends more boxes onto the best-paying paths but also reshapes refueling to avoid weight interference on those paths.

S3 (Localized price at A). Changing the fuel price at port A alone isolates the value of a single cheap or expensive bunkering location while holding all other ports and all leg consumptions fixed. When the price at A is discounted, both approaches bunker more at that port; when it is marked up, both approaches bunker less there and shift purchases to nearby ports. The key difference is how far to push the initial purchase when the price is low and how to rebalance when the price is high. The two-stage model tends to over-concentrate purchases at A in the discount case because it optimizes fuel cost without considering cargo yet; this creates unnecessary fuel carry into heavy legs and reduces payload for high-margin containers. The integrated model exploits the discount but caps carry on the heavy segments by postponing part of the purchase to later legs with more slack. In the markup case it reallocates even more aggressively to protect revenue on the critical legs. Table 3 shows an almost linear decline in profit as the multiplier at A rises from 0.8 to 1.2, with a total loss of about 1.70 M USD for the two-stage model and about 1.60 M USD for the integrated model. The premium of the integrated over the two-stage model remains stable, approximately 2.6–3.0 M USD across the tested range. Practically, this indicates that a single-port shock can be buffered by distributing purchases across the cycle and by re-timing fuel so that the heaviest legs carry less fuel weight. It also shows that contract advantages at one port have an optimum: beyond that point, extra early purchases depress revenue by inflating carried fuel on heavy legs. The integrated model identifies that turning point endogenously, whereas a

bunker-first policy risks crossing it and losing more profit than it saves on fuel.

4.2.4. Computational performance, solution quality and scalability

Beyond economic performance, the practical value of an optimization model depends on its ability to be solved reliably within operationally acceptable time limits. In liner shipping applications, such models are typically embedded in weekly or even daily planning cycles, where solution delays of more than a few minutes can hinder adoption. It is therefore important not only to compare the economic outcomes of the two formulations, but also to document their computational behaviour under a transparent and reproducible setup.

To this end, we implemented both the two-stage and integrated formulations in Python using the PuLP modeling interface and solved them with the CBC mixed-integer linear programming solver. All instances were run on a standard desktop computer equipped with an Intel i7 CPU and 16 GB of RAM, without any problem-specific code optimization, decomposition, or warm-start procedures. The reported CPU times thus provide indicative orders of magnitude for a “generic” implementation, rather than best-possible performance under tailored algorithmic enhancements. Table 4 summarizes the average wall-clock times over multiple runs for each instance.

Table 4. Indicative CPU time for each instance.

Instance	CPU time (s)
3-port, two-stage	0.1
3-port, integrated	0.2
8-port, two-stage	1.0
8-port, integrated	1.6
15-port, two-stage	5.2
15-port, integrated	8.4

Several observations can be drawn from Table 4. First, for all three instance sizes, both formulations are solved to optimality within seconds or, for the largest case, within a few seconds. This confirms that, for the problem scales considered in our numerical experiments (3, 8, and 15 ports with two routes), the integrated formulation does not introduce prohibitive computational overhead. In particular, the jump from the two-stage to the integrated model increases CPU time, but only by a moderate factor (approximately 1.2–1.6 across instances), which is negligible in typical tactical planning horizons.

Second, because both models are linear and solved with an exact branch-and-bound-based solver, the reported CPU times correspond to globally optimal solutions for the stated formulations. There is therefore no explicit trade-off between solution quality and computation time in this setting: a planner does not need to sacrifice optimality to obtain the improvements associated with the integrated approach. This stands in contrast to many large-scale network design or crew scheduling problems, where near-optimal solutions are often accepted due to time limits. In our case, the integrated model delivers both higher profit and exact optimality at an additional computational cost that remains modest for the tested network sizes.

Third, the growth in CPU time as the problem size increases from 3 to 8 and 15 ports is in line with the expected increase in the number of variables and constraints, and with the more complex structure of the 15-port network. The two-stage model, which decouples bunkering and stowage, benefits slightly

from a smaller effective search space, whereas the integrated model solves a single larger problem that captures all interactions explicitly. Even so, the 15-port integrated instance is solved in under 10 seconds in our basic implementation, suggesting that networks somewhat larger than those studied here (e.g., 20–25 ports) would still be tractable on standard hardware, especially if modern commercial solvers or modest problem-specific enhancements (e.g., presolving, tighter bounds, and warm-starts from two-stage solutions) are used.

At the same time, it is important to emphasize that the times reported in Table 4 are indicative rather than prescriptive. Actual runtimes will depend on the choice of solver, implementation language, hardware configuration, and the exact parameterization of a real shipping service (e.g., number of OD pairs, number of routes, or inclusion of additional constraints such as time windows or transshipment). As the model is enriched along these dimensions, decomposition schemes (e.g., Benders-type cuts in the space of bunker and flow decisions) or customized heuristics may be useful to maintain near-real-time performance for very large-scale networks.

Overall, these computational results show that the proposed integrated refueling-and-routing formulation is not only conceptually appealing and economically advantageous, but also practically implementable within the time budgets typical of tactical liner shipping planning. The modest increase in CPU time relative to the two-stage benchmark is small compared with the profit gains documented in the previous subsections, supporting the view that integrated planning can be adopted as a routine decision-support tool rather than only as an offline benchmarking device.

5. Conclusions

5.1. Principal findings

This paper compares a sequential *two-stage* approach, which fixes bunkering decisions before cargo assignment, with an *integrated* approach that jointly optimizes refueling and container flows. Based on three benchmark instances (3, 8, and 15 ports) under consistent capacity, demand and price settings, the main conclusions can be summarized as follows.

- 1) The integrated model yields higher network profit in all instances.
- 2) The profit improvement is not only due to lower fuel expenditure but also to a more effective *placement* of fuel in time and space. By aligning purchase timing and quantities with cargo flows, the integrated solution reduces carried fuel on fuel-intensive, revenue-critical legs and releases weight for high-yield origin–destination movements.
- 3) Sensitivity experiments on the 8-port network show that these advantages are robust. Enlarging tank capacity produces monotone but diminishing profit gains, with a larger benefit for the integrated model; scaling all revenues leads to almost proportional profit growth, again with higher profit elasticity for the integrated model; and a localized price shock at a single port reduces profits for both models but is better absorbed by the integrated solution, which maintains an approximately 2.6–3.0 MUSD advantage across the tested range.
- 4) Given typical cost structures and profit margins in liner shipping, the observed profit improvements of roughly 9–13% in the larger instances represent economically meaningful gains that could materially enhance voyage profitability when applied systematically across services.

5.2. Limitations

There are still several limitations in this study that qualify the interpretation of the results. First, to isolate the economic value of integration and obtain clear comparative statics, the analysis relies on deterministic demands and bunker prices within each weekly cycle, exogenous port visitation times and sailing speeds, fixed per-leg consumption profiles, and a single service without transshipment or fleet interactions. These assumptions simplify the problem and make it possible to attribute performance differences directly to the modeling structure, but they also abstract from several sources of operational complexity.

In particular, demand and price uncertainty may affect the relative advantage of the integrated model. If high bunker prices tend to coincide with high demand on certain corridors, the ability to coordinate refueling and cargo allocation could become even more valuable, strengthening the case for integration. Conversely, if the operator adopts strongly risk-averse policies or faces highly volatile spot markets, part of the benefit of a deterministic integrated solution might be eroded and replaced by the value of flexibility or optionality in refueling contracts. From a practical viewpoint, a two-stage decomposition may also be easier to embed in rolling planning processes with frequent demand updates, whereas a fully integrated model would benefit from more stable forecast inputs.

The absence of explicit congestion, berth-capacity constraints, and time windows also has implications. In this study, capacity conflicts arise only through deadweight and slot limits; in reality, schedule reliability and quay-side resources may restrict the extent to which flows can be rebalanced in favor of certain ports or corridors. Introducing such constraints could moderate the integrated model's ability to reshuffle cargo and refueling across ports, potentially reducing—but not eliminating—the profit gap relative to the two-stage approach.

Finally, the numerical experiments are based on systematically generated, stylized instances calibrated to typical liner shipping parameters rather than on a single real-world case study or publicly available benchmark network. While this design ensures transparency and reproducibility, it also means that the quantitative magnitude of the reported profit gains should be interpreted as indicative rather than definitive for any specific service. A more thorough external validation against proprietary operational data or standardized test sets is therefore needed before firm-level implementation.

5.3. Future research

Several extensions follow naturally from the present work and build directly on the proposed formulations.

A first direction is to consider joint speed-bunkering-stowage planning. By incorporating speed choice and convex fuel-speed relationships via piecewise-linear approximations, the model can be used to study trade-offs between time, fuel, and weight on critical legs, while preserving the same basic structure of the integrated formulation. This would allow a unified assessment of slow steaming, bunker procurement and cargo allocation decisions.

A second direction is to introduce demand and price uncertainty through explicit stochastic or robust counterparts. For example, one could formulate a two-stage stochastic program in which first-stage decisions fix refueling contracts and base-route structures, while second-stage recourse decisions adjust port-level bunkering and container flows under a finite set of demand and price scenarios. Alternatively, distributionally robust variants could be calibrated to historical bunker quotes and booking records, and

solved by decomposition methods that exploit the refuel–stowage block structure of the present model.

A third direction is to include time-dependent operations, such as berth-capacity and time-window constraints, by embedding the current network in a time-expanded graph. Simple queueing-based delay penalties or service-level constraints could then be added to the objective and constraints, and rolling-horizon schemes could be evaluated that re-solve the integrated model at each port call using updated state information.

In addition, the procurement structure can be enriched by endogenizing contract design (volume commitments, indexed collars and minimum-lift clauses) alongside spot purchases, so that the model chooses not only where and when to bunker but also how to allocate volume across instruments. Building on the present integrated formulation, such an extension would quantify the value of contract flexibility relative to purely spot-based strategies. The framework can also be extended to interacting services with transshipment, in order to examine whether cross-loop coordination yields further economies of scope.

Finally, an important practical step is to calibrate and test the models on real-world services or publicly documented benchmark networks. This would involve mapping actual port rotations, bunker contracts and OD demand data into the model parameters, and comparing the integrated and two-stage solutions against current operating practices in terms of both economic performance and implementability.

5.4. Overall summary

Within the above scope, this study provides quantitative evidence that integrated planning in liner shipping can bring economically meaningful and scalable improvements over sequential bunkering–then–stowage planning, and that these benefits persist under a range of operational, market, and input-cost perturbations. As liner services face tighter energy, carbon and reliability constraints, such integrated models offer a useful tool for improving the joint use of fuel and cargo capacity, and the proposed extensions indicate a concrete path toward applications in data-rich and time-sensitive operational environments.

Use of AI tools declaration

The authors declare they have not used Artificial Intelligence (AI) tools in the creation of this article.

Acknowledgment

This work was supported by the Research Grants Council of the Hong Kong Special Administrative Region, China [Project Number 15508722].

Conflict of interest

The authors declare there is no conflicts of interest.

References

1. B. Li, P. Afkhami, R. Khayamim, M. Borowska-Stefańska, S. Wiśniewski, A. M. Fathollahi-Fard, et al., An intelligent hyperheuristic algorithm for the berth allocation and scheduling problem at marine container terminals, *Transp. Res. Part E Logist. Transp. Rev.*, **198** (2025), 104104. <https://doi.org/10.1016/j.tre.2025.104104>
2. M. Mollaoglu, I. G. Yazar Okur, M. Gurturk, B. Doganer Duman, Review on Sustainable Development Goals in maritime transportation: current research trends, applications, and future research opportunities, *Environ. Sci. Pollut. Res.*, **31** (2024), 8312–8329. <https://doi.org/10.1007/s11356-023-31622-1>
3. A. Ala, A. Goli, Incorporating machine learning and optimization techniques for assigning patients to operating rooms by considering fairness policies, *Eng. Appl. Artif. Intell.*, **136** (2024), 108980. <https://doi.org/10.1016/j.engappai.2024.108980>
4. M. Y. N. Attari, A. Ala, V. Simic, D. Pamucar, N. Aydin, A gravitational meta-heuristic algorithm for solving resource-constrained project scheduling problems, *Sadhana - Acad. Proc. Eng. Sci.*, **50** (2025), 104. <https://doi.org/10.1007/s12046-025-02745-7>
5. M. Besbes, S. Savin, Going bunkers: The joint route selection and refueling problem, *Manuf. Serv. Oper. Manag.*, **11** (2009), 694–711. <https://doi.org/10.1287/msom.1080.0249>
6. K. Fagerholt, G. Laporte, I. Norstad, Reducing fuel emissions by optimizing speed on shipping routes, *J. Oper. Res. Soc.*, **61** (2010), 523–529. <https://doi.org/10.1057/jors.2009.77>
7. S. Wang, Q. Meng, Robust bunker management for liner shipping networks, *Eur. J. Oper. Res.*, **243** (2015), 789–797. <https://doi.org/10.1016/j.ejor.2014.12.049>
8. T. Wang, P. Cheng, L. Zhen, Green development of the maritime industry: Overview, perspectives, and future research opportunities, *Transp. Res. Part E Logist. Transp. Rev.*, **179** (2023), 103322. <https://doi.org/10.1016/j.tre.2023.103322>
9. Q. Meng, S. Wang, Liner shipping service network design with empty container repositioning, *Transp. Res. Part E Logist. Transp. Rev.*, **47** (2011), 695–708. <https://doi.org/10.1016/j.tre.2011.02.004>
10. Y. Wang, Q. Meng, Y. Du, Y. Zhao, Liner shipping network design with deadlines, *Comput. Oper. Res.*, **41** (2014), 140–149. <https://doi.org/10.1016/j.cor.2013.06.010>
11. S. Wang, Q. Meng, Robust schedule design for liner shipping services, *Transp. Res. Part E Logist. Transp. Rev.*, **48** (2012), 1093–1106. <https://doi.org/10.1016/j.tre.2012.04.007>
12. D. Ronen, The effect of oil price on the optimal speed of ships, *J. Oper. Res. Soc.*, **33** (1982), 1035–1040. <https://doi.org/10.1057/jors.1982.215>
13. E. E. Halvorsen-Weare, K. Fagerholt, L. M. Nonås, B. E. Asbjørnslett, Optimal fleet composition and periodic routing of offshore supply vessels, *Eur. J. Oper. Res.*, **223** (2012), 508–517. <https://doi.org/10.1016/j.ejor.2012.06.017>
14. Y. Du, Q. Meng, S. Wang, H. Kuang, Two-phase optimal solutions for ship speed and trim optimization over a voyage using voyage report data, *Transp. Res. Part B Methodol.*, **122** (2019), 88–114. <https://doi.org/10.1016/j.trb.2019.02.004>

15. H. Psaraftis, C. Kontovas, Speed models for energy-efficient maritime transportation: A taxonomy and survey, *Transp. Res. Part C Emerg. Technol.*, **26** (2013), 331–351. <https://doi.org/10.1016/j.trc.2012.09.012>
16. J. E. Korsvik, K. Fagerholt, G. Laporte, A tabu search heuristic for ship routing and scheduling, *J. Oper. Res. Soc.*, **61** (2010), 594–603. <https://doi.org/10.1057/jors.2008.192>
17. L. Zhen, S. Wang, D. Zhuge, Dynamic programming for optimal ship refueling decision, *Transp. Res. Part E Logist. Transp. Rev.*, **100** (2017), 63–74. <https://doi.org/10.1016/j.tre.2016.12.013>
18. S. Wang, Q. Meng, Z. Liu, Bunker consumption optimization methods in shipping: A critical review and extensions, *Transp. Res. Part E Logist. Transp. Rev.*, **53** (2013), 49–62. <https://doi.org/10.1016/j.tre.2013.02.003>
19. S. Xie, Z. Hu, J. Wang, Scenario-based comprehensive expansion planning model for a coupled transportation and active distribution system, *Appl. Energy*, **255** (2019), 113782. <https://doi.org/10.1016/j.apenergy.2019.113782>
20. T. Gerres, J. P. C. Ávila, P. L. Llamas, T. G. San Román, A review of cross-sector decarbonisation potentials in the European energy intensive industry, *J. Clean. Prod.*, **210** (2019), 585–601. <https://doi.org/10.1016/j.jclepro.2018.11.036>
21. L. Fan, W. W. Wilson, B. Dahl, Congestion, port expansion and spatial competition for US container imports, *Transp. Res. Part E Logist. Transp. Rev.*, **48** (2012), 1121–1136. <https://doi.org/10.1016/j.tre.2012.04.006>
22. C. E. M. Plum, P. N. Jensen, D. Pisinger, Bunker purchasing with contracts, *Marit. Econ. Logist.*, **16** (2014), 418–435. <https://doi.org/10.1057/mel.2014.15>
23. S. Devarapali, A. Manske, R. Khayamim, E. Jacobs, B. Li, Z. Elmi, et al., Electric tugboat deployment in maritime transportation: detailed analysis of advantages and disadvantages, *Marit. Bus. Rev.*, **9** (2024), 263–291. <https://doi.org/10.1108/MBR-09-2023-0067>



AIMS Press

©2026 the Author(s), licensee AIMS Press. This is an open access article distributed under the terms of the Creative Commons Attribution License (<https://creativecommons.org/licenses/by/4.0>)